Physics of the Solid State, 2022, Vol. 64, No. 7

09,04

A Low-wavelength host absorption edge of LiB_3O_5 and $Li_2B_4O_7$ crystals

© *I.N. Ogorodnikov*

Ural Federal University after the first President of Russia B.N. Yeltsin,
Yekaterinburg, Russia

E-mail: i.n.ogorodnikov@urfu.ru

Received March 14, 2022
Revised March 14, 2022
Accepted March 15, 2022

We have carried out an experimental study of the VUF- edge of the optical host absorption of lithium borate crystals LiB_3O_5 (LBO) and $Li_2B_4O_7$ (LTB). The transmission ($T = 293$ K) and absorption ($T = 80, 293$ K) spectra were studied, the short-wavelength edge of the transparency band (cutoff wavelength) and the energy position of the edge fundamental absorption at which the absorption coefficient $k = 50\,\mathrm{cm}^{-1}$ were determined. The absorption edge temperature shift coefficient $-(3-4.7) \cdot 10^{-4}$ eV/K was determined. The dependence of the absorption edge parameters of oriented LBO $\perp Y$ and LBO $\perp X$ crystals has been studied. Based on low-temperature reflection spectra ($T = 10$ K, $\theta = 17^\circ$, $E = 4-32$ eV) the Kramers–Kronig method was used to calculate the spectra of optical constants: refractive index (n) and absorption index (k), real (ε_1) and imaginary (ε_2) parts of the complex permittivity, as well as the absorption coefficient μ. The lowest energy peak, due to electronic transitions from the top of the valence band to the states of the bottom of the conduction band, was studied in the $\varepsilon_2(E)$ spectrum, the thresholds for interband transitions were determined (E_g at $T = 10$ K): 8.5–8.6 eV(LBO $\perp Y$), 8.6–8.7 eV (LBO $\perp X$) and 8.8–8.9 eV (LTB). The origin of the fundamental absorption edge of lithium borates is discussed.

Keywords: Lithium triborate LiB_3O_5, lithium tetraborate $Li_2B_4O_7$, host absorption edge, optical properties.

DOI: 10.21883/0000000000

1. Introduction

Defect-free, undoped optical materials are relatively transparent to photons whose energy $h\nu$ does not exceed a certain threshold energy associated with the energy threshold of interband transitions E_g, or with the energy threshold of direct excitation of free excitons [1]. Thus, a typical germanium semiconductor in the optical transparency band can have an absorption coefficient of $k < 0.1\,\mathrm{cm}^{-1}$, but when $h\nu \to E_g$, the values k rapidly increase up to $10^4-10^5\,\mathrm{cm}^{-1}$ in a narrow energy range of 0.1 eV [2]. The energy interval of a sharp increase k is called the long-wavelength fundamental absorption edge or simply the fundamental absorption edge.

The nature of fundamental absorption is determined by induced transitions from the valence band to the conduction band or to exciton states located near (below) the bottom of the conduction band. The study of the fundamental absorption edge provides valuable information about the edge of the optical transparency band, exciton states, electronic states of the bottom of the conduction band and the top of the valence band, as well as data on the nature and quantitative characteristics of the probabilities of optical transitions. The information obtained as a result of studying the fundamental absorption edge is of particular value, since it is the states immediately adjacent to the band gap that determine most of the optical, laser, and electrical characteristics of an optical material.

Low symmetry optical crystals are widely used in modern shortwave laser optics as nonlinear converters, parametric oscillators and other nonlinear optical elements [3]. From the crystallographic point of view, such crystals are characterized by a complex lattice cell containing several formula units, which is tens and hundreds of atoms.

Nonlinear optical crystals of lithium tetraborate $Li_2B_4O_7$ (LTB) and lithium triborate LiB_3O_5 (LBO) are of considerable interest from this point of view: they are characterized by a wide optical transparency band (165–5500 nm and 159–3500 nm, respectively), the short-wavelength boundary of which is located in the vacuum ultraviolet (VUV) region, with high efficiency of non-linear-optical conversion, high radiation resistance to high-power ($\mathrm{GW/cm^2}$) laser radiation. LBO crystals belong to the orthorhombic crystal system ($Pna2_1$) with lattice parameters $a = 0.8447$ nm, $b = 0.7379$ nm, $c = 0.5141$ nm. The main structural motif — anionic group — consists of a tetrahedron BO_4 and two non-equivalent trigonal structures BO_3; the lattice cell contains 4 formula units (36 atoms). LTB crystals belong to the tetragonal crystal system ($I4_1cd$) with lattice parameters $a = b = 0.9477$ nm, $c = 1.0286$ nm. The structural motif is represented by two equivalent tetrahedra and two equivalent trigonal structures; the elementary cell contains 8 formula units (104 atoms). In both LTB and LBO crystals, the anionic groups are exactly joined to each other, forming a continuous boron-oxygen framework in each of the crystals. Lithium atoms are located in the voids of the framework and play the role of structure stabilizers.

Prior to our work, there were very limited data on the reflection spectra of lithium borate crystals. Thus, for LTB in the range 6−18 eV the c were measured at 290 K and the optical constants [4,5] were calculated by the Kramers−Kronig method; the reflection spectra were measured at $T = 10$ K, in the range 5−20 eV without reference to absolute values [6]. For LBO at 290 K in the range 6−12 eV the reflection spectra were measured and the optical constants [7] were calculated on the basis of the oscillator model.

The purpose of this article is to experimentally study the VUV- of the fundamental optical absorption edge of lithium borate crystals LTB and LBO, to obtain quantitative characteristics using optical VUV-spectroscopy, including the calculation of optical constants based on low-temperature ($T = 10$ K) reflection spectra measured in a wide range of photon energies 4−33 eV.

2. Research targets and methods

We used single crystals LTB and LBO of optical quality grown at the Institute of Geology and Mineralogy of the Siberian Branch of the Russian Academy of Sciences (Novosibirsk) by the solution-melt method, the growth technology of which is described in [8]. For spectroscopic studies, we used samples of intentionally undoped (nominally pure) LTB and LBO crystals $8 \times 8 \times 1$ mm in size with polished planar parallel surfaces. The planes of the LBO samples were perpendicular to the crystallographic axes X or Y (LBO $\perp X$ and LBO $\perp Y$), the LTB samples were not oriented.

Optical measurements were performed on an experimental setup, which includes a vacuum monochromator BMP-2 with a spherical grating of 600 lines/mm, a high-aperture monochromator MDR-2 with a grating of 1200 lines/mm; photomultipliers FEU-106 and FEU-142 operating in the photon counting mode; VMF-25 hydrogen lamp as a source of optical radiation in the vacuum ultraviolet (VUV) region; a vacuum optical chamber with MgF_2 windows, equipped with a fast-response cryostat with interchangeable units for operation in a wide temperature range from $T = 10$ to 600 K, and means of oil-free pumping. Spectra of optical transmission (T) and optical absorption (k) are obtained using the following relations:

$$T(E) = \frac{I(E)}{I_0}; \quad k(E) = -\frac{1}{d}\ln(T), \tag{1}$$

where I_0 is intensity of the incident beam; $I(E)$ is intensity of the transmitted beam; E is photon energy; d is sample thickness in cm. Optical transmission T is the ratio of two quantities of the same type and therefore it is presented in dimensionless units, or as a percentage. Optical absorption k has dimension of cm^{-1}.

Low-temperature ($T = 10$ K, $\theta = 17°$, $E = 4{-}33$ eV) were measured in our earlier article [9] and are presented in it without reference to the absolute values of the reflection coefficient. The article [9] gives all the necessary details of the experiment, we only note that the primary monochromator with a platinum-coated diffraction grating provided a spectral resolution of 0.32 nm in the energy range of 4−40 eV. In this article, reference was made to the absolute values of the reflection coefficient by the Fresnel relations based on the known dispersion of the refraction indices of LTB and LBO in the visible region of the spectrum [10–12].

3. Experimental results

3.1. Transmission and absorption spectra

Figure 1, a shows fragments of the transmission spectra of LTB and LBO crystals at room temperature, measured in the UV−VUV-region of the spectrum without correction for reflection. In the wavelength range from 260 to 175 nm, the transmission spectra of both crystals are represented by even, almost horizontal lines without any dips. With a further decrease in the wavelength, a sharp decrease in the ccrystals transparency to zero is observed, which begins approximately at 170 nm for LTB and 165 nm for LBO.

To characterize the short-wavelength boundary of the crystal transparency region, we will use the cutoff wavelength λ_c. To determine it, the $T(\lambda)$ spectrum in the region of a sharp transparency decrease is approximated by a straight line, which extrapolation to the intersection with the abscissa gives the value $\lambda = \lambda_c$. In our measurements, the following values λ_c were obtained: 159 nm (LBO $\perp X$), 156 nm (LBO $\perp Y$) and 165 nm (LTB), which are in good agreement with the results of earlier articles [13–16].

Figure 1, b shows the optical absorption spectra of initial unirradiated LTB and LBO lithium borate crystals measured in the UV−VUV-spectral region at temperatures $T = 80$ (LBO) and 293 K (LBO, LTB). At the same time, the LBO samples were in different crystal-lattice orientation: the sample plane was perpendicular to the X axis (LBO $\perp X$) or the Y axis (LBO $\perp Y$). In the transparency region of all samples (LTB, LBO of both orientations), no optical absorption bands were found. Two energy parameters were used to describe the absorption edge: E_1 is energy at which the coefficient is $k \approx 3\,\mathrm{cm}^{-1}$ and E_2 is energy at which the coefficient is $k \approx 50\,\mathrm{cm}^{-1}$. At $E < E_1$, each of the spectra demonstrates unstructured background absorption not exceeding $3\,\mathrm{cm}^{-1}$. At $E > E_1$, a monotonic exponential increase in the absorption coefficient is observed, which occurs in a relatively narrow energy range. The formal characteristics of this portion of the absorption spectrum in each of the crystals are comparable to those for the VUV-fundamental absorption edge. Anisotropy of the VUV-absorption edge is observed for the LBO crystal: at the absorption coefficient level $k(E_2) = 50\,\mathrm{cm}^{-1}$ the absorption edge LBO $\perp Y$ is shifted to the shortwave region by 170 meV (293 K) and 180 meV (80 K) as compared to that for LBO $\perp X$. Note that in both cases the crystallographic axis 2_1 was perpendicular to the direction of probing light propagation. Cooling the crystal from

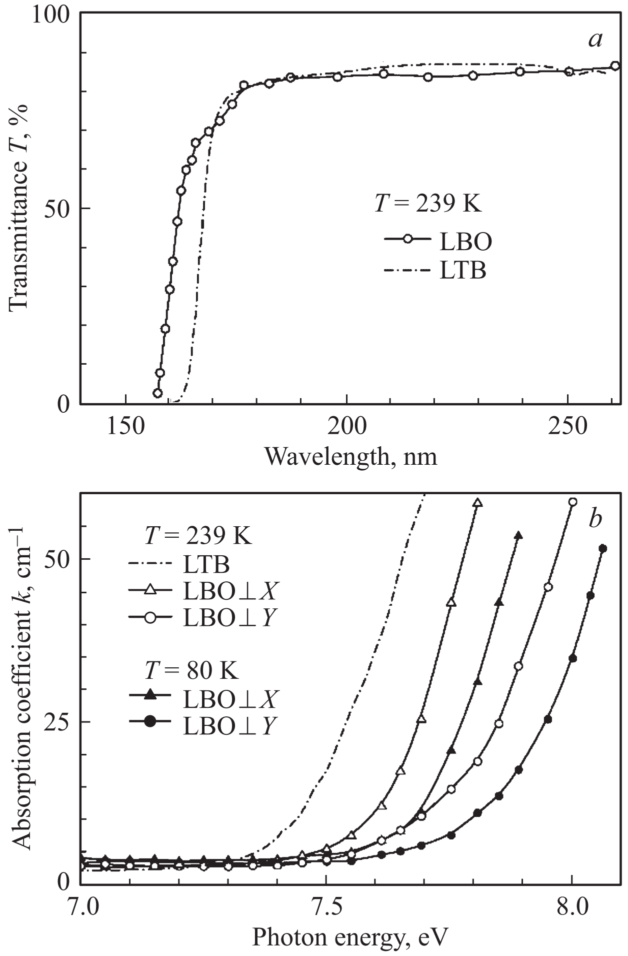

Figure 1. Optical transmission (*a*) and absorption (*b*) spectra of LTB and LBO crystals, measured in the VUV-region of the fundamental absorption edge of crystals.

room temperature to 80 K also leads to a short-wavelength shift of the LBO fundamental absorption edge by 90 meV ($\text{LBO} \perp X$) and 100 meV ($\text{LBO} \perp Y$). Note that the cutoff wavelength λ_c corresponds to the energy at which $k \approx 20-50\,\text{cm}^{-1}$.

3.2. Spectra of optical constants

Figure 2 shows the reflection spectra $R(E)$ of LTB and LBO crystals at 9.6 K measured over a wide energy range 7–35 eV. For all the reflection spectra obtained, attention is drawn to the relatively small value of the reflection coefficient, the absence of sharp intense peaks characteristic of the exciton structure of the reflection spectra, and the significant similarity of the LTB and LBO reflection spectra. As the photon energy changes from the transparency region, the reflection coefficient of both crystals increases monotonically, above the absorption edge it reaches the first broad maximum at 9–10 eV. The absolute maximum in the reflection spectra is observed in the region of 15–16 eV, then, as the energy changes to 30 eV, a smooth monotonic decrease in the reflection coefficient occurs.

Based on the experimental reflection spectra, we have calculated the spectra of the LTB and LBO optical constants using the difference method of Kramers–Kronig integral relations, which is described in the classical article [17]. Note that the low-temperature reflection spectra $R(E)$ were obtained by us for both crystal orientations $\text{LBO} \perp Y$ and $\text{LBO} \perp X$. The spectra of optical constants were also calculated for both orientations. However, due to the significant qualitative similarity of all these spectra, Figures 2 and 3 show spectra for only one $\text{LBO} \perp X$ orientation, and all quantitative differences between these spectra are discussed in the text if necessary.

Figure 2 shows the calculated spectra of optical functions n (refraction index) and k (absorption index) obtained by processing low-temperature reflection spectra $R(E)$ using the Kramers–Kronig method. It can be seen in Fig. 2 that in the spectrum $n(E)$ the long-wave maximum is located at 9.5 eV (LTB) and 9.1–9.3 eV (LBO), followed by a minimum at 10.7–10.8 eV, second maximum at 12.4–12.5 eV and arm at 13.8–14.0 eV. A detailed examination also revealed the presence of a low-intensity arm in the region of 8.4 eV. It is of interest to determine the energy at which

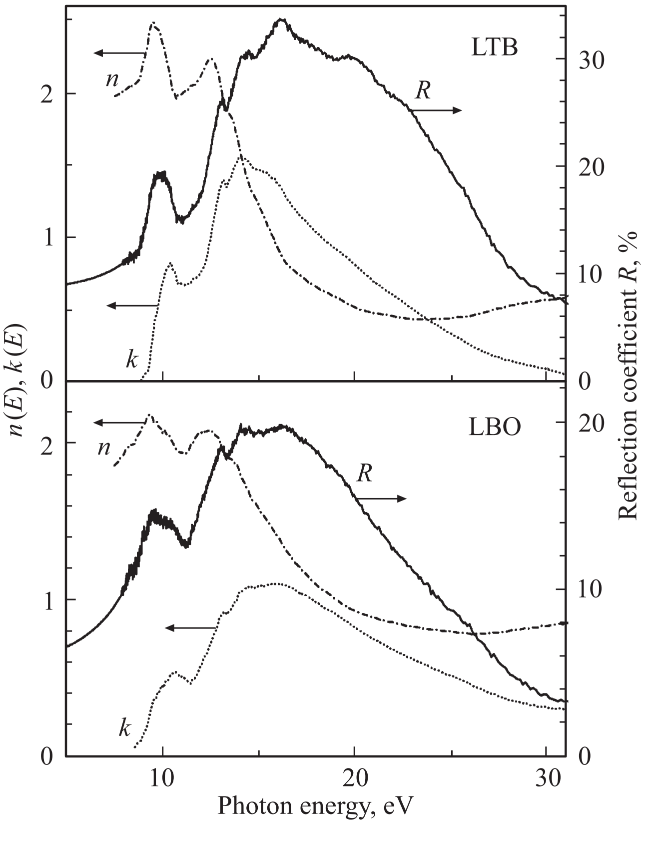

Figure 2. Reflection spectra (R) of LTB and LBO crystals ($T = 9.6\,\text{K}$, $\theta = 17°$); calculated spectra of optical functions n and k obtained by processing $R(E)$ using the Kramers–Kronig method.

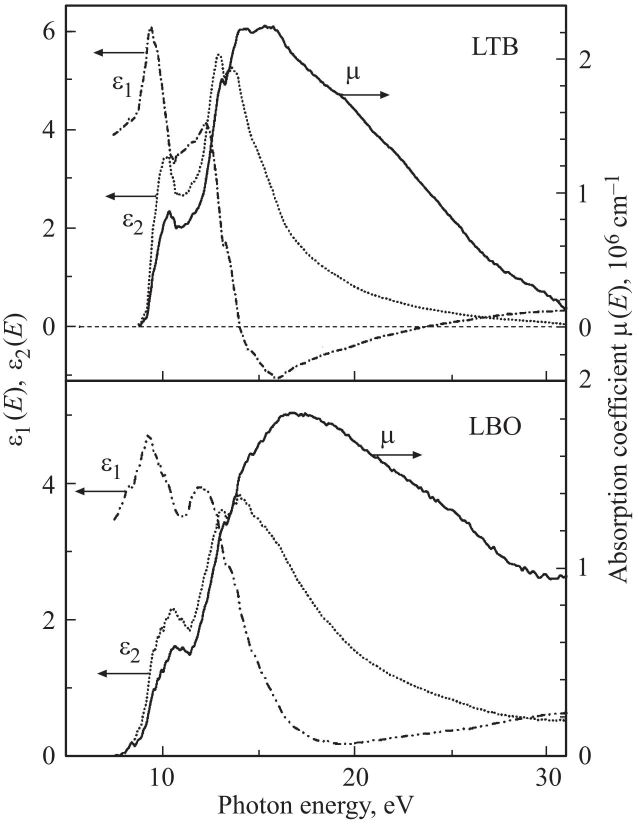

Figure 3. Calculated spectra of optical functions $\varepsilon_1, \varepsilon_2$ and μ obtained by processing $R(E)$ using the Kramers–Kronig method.

the falling value $n(E) = 1$. The sum rule [18] is known:

$$\int_0^\infty [n(E) - 1]dE, \tag{2}$$

from which it follows that the average refraction index value over the entire energy range is equal to unity, and the parts of the curve $[n(E)-1]$ below and above the abscissa must have the same areas. It follows from our data (Fig. 2) that the boundary points, where $n(E) = 1$, are 15.7 eV (LTB), 19.0 eV (LBO $\perp Y$) and 19.4 eV (LBO $\perp X$).

Based on the obtained optical functions $n(E)$ and $k(E)$, other optical functions were calculated: real (ε_1) and imaginary (ε_2) components of the complex permittivity $\varepsilon = \varepsilon_1 + i\varepsilon_2$, as well as the absorption coefficient $\mu(E)$:

$$\varepsilon_1 = n^2 - k^2,$$

$$\varepsilon_2 = 2nk,$$

$$\mu = 4\pi k/\lambda, \tag{3}$$

where λ is wavelength of the incident light, cm^{-1}.

Figure 3 shows the spectra of the optical functions $\varepsilon_1(E)$, $\varepsilon_2(E)$, and $\mu(E)$. Spectrum $\varepsilon_2(E)$ is one of the most important optical functions, its structure and shape are determined by the position of critical state density points. In the region of fundamental absorption, the spectrum is characterized by a number of peaks in the 8–12 eV region and a wide band in the 12–16 eV region. The lowest energy peak $\varepsilon_2(E)$ in LTB and LBO crystals is observed near 10.4–10.6 eV, however, an arm is observed in the 9.6–10 eV region. At energies above 11.3–11.4 eV, $\varepsilon_2(E)$ rises sharply with a double maximum in the 13–14 eV region. In the energy region above 14 eV, the function $\varepsilon_2(E)$ monotonic decrease is observed, which corresponds to the depletion of the sum rule and may indicate the plasma oscillation excitation in the valence band. The absorption spectrum of $\mu(E)$ in the region 8.9–14.0 eV (LTB) and 8.9–16.0 eV (LBO) shows a steeply increasing curve whose structural features correspond to those for $\varepsilon_2(E)$. A wide flat maximum takes place in the region 14–16 eV (LTB) or 16–17.5 eV (LBO). The absorption coefficient at the $\mu(E)$ maximum reaches $2.2 \cdot 10^6\,cm^{-1}$ (LTB) and $1.8 \cdot 10^6\,cm^{-1}$ (LBO). Further, a smooth monotonic decrease of $\mu(E)$ is observed. The $n(E)$ and $\mu(E)$ spectra obtained by us for the LBO crystal (Figs. 2 and 3) are quite comparable in profile and absolute values with the theoretical spectra of $n(E)$ and $\mu(E)$ calculated in the article [19] on the basis of band calculations of the electronic structure LBO.

4. Discussion of results

Results of numerous band [19–22] and cluster [23–25] calculations of the electronic structure of LTB and LBO, as well as X-ray photoelectron spectroscopy data for these crystals [20,25,26] unambiguously indicate that the electronic structure of the lithium borates valence band is formed mainly by anionic states. In this case, boron ions make only a relatively small contribution to the formation of the states of the valence band and the conduction band, while the lithium ions states do not contribute to the electronic structure of the valence band of the crystal. In this regard, the electronic states of lithium borates are determined by localized boron-oxygen bonds. It also follows from the calculations that the lithium borates bands have a small dispersion in the k- space and, in particular, the valence band has minigap in the entire range of the wave vector. As a result, the effective mass of charge carriers is quite large and is estimated at $0.73m_e$, $0.89m_e$ and $0.69m_e$ for the directions of the conduction band Γ — X, Γ — S, Γ — Z respectively [22].

Analysis of possible electronic transitions from the upper valence band to the lower conduction band showed that they are determined by the electronic structure of the boron-oxygen groups, and this situation is typical for lithium borates, as well as CsB_3O_5 (CBO) and β-BaB_4O_7 (BBO). Calculation of the electronic structure of these crystals by the zone method of linearized augmented plane waves [19] showed that the top of the valence band in all crystals is formed predominantly by oxygen orbitals with an almost complete absence of the contribution from boron ions. In this case, the lowest energy electronic transition in lithium borates occurs to states formed by hybridized orbitals of trigonally coordinated boron and oxygen ions, which form the bottom of the conduction band.

Unlike alkali-halide crystals [27] and some binary oxides (for example, BeO [28]), the study of lithium borates in the low-temperature ($T = 10\,\mathrm{K}$) region [9] did not reveal any luminescent manifestations of these states near the fundamental absorption edge. This picture is typical for some simple oxides (for example, in MgO, $\mathrm{Al_2O_3}$) and, apparently, takes place in BBO [29] and LTB [6]. This interpretation is supported by the shape of the excitation spectrum of the lithium borates luminescence excited in the crystal fundamental absorption region, which is typical for crystals with an exciton luminescence character, its characteristic temperature dependence, a large emission band width, and a significant Stokes shift. In the article [9] LBO luminescence is attributed to radiative annihilation of relaxed exciton-like electronic excitations, as is the case in BBO [29] or LTB [6] crystals, or to the emission of relaxed excitons localized on insignificant structural distortions [30].

Theoretical E_g estimates for lithium borates give the values $7.75-7.80\,\mathrm{eV}$ [20,21,23]. At the same time, according to [22], the band calculation of the LBO electronic structure predicts a band gap of 7.37 eV in the $\Gamma-\Gamma$ direction. Calculations [7,31] based on the analysis of LBO reflection spectra measured in the $6-12\,\mathrm{eV}$ region give a value of 7.3 eV for the highest vacant orbital $4a_2$ referred to the states of the band bottom conductivity. However, according to our experimental data (Fig. 1), all these theoretical estimates of E_g of lithium borates fall within the energy range from E_1 to E_2, i.e., in the region of the absorption edge, where the absorption coefficient does not exceed $50\,\mathrm{cm}^{-1}$. This does not allow us to agree with the theoretical estimates of the band gap of lithium borates, since the expected value of the absorption coefficient in the E_g region should be much higher: $10^4-10^6\,\mathrm{cm}^{-1}$.

The spectra $\varepsilon_2(E)$ of the imaginary part of the complex permittivity of lithium borates obtained in this article give grounds for a more adequate estimate of E_g. Indeed, the lowest-energy peak in the $\varepsilon_2(E)$ spectrum is usually compared with the lowest-energy electronic transitions from the top of the valence band to states at the conduction band bottom, so the threshold for interband transitions E_g can be estimated as the cutoff energy of the low-energy peak $\varepsilon_2(E)$.

For each of the LTB and LBO crystals, Figure 4 shows a fragment of the dependence of $E\sqrt{\varepsilon_2}$ on the energy E constructed for the energy region near the absorption edge of the corresponding crystal. It can be seen in Fig. 4 that as the photon energy increases, the background absorption level is replaced by an increasing absorption represented by a straight line, which shows that the following dependence [32]: takes place in this energy range:

$$E^2\varepsilon_2 \propto (E - E_g)^2. \tag{4}$$

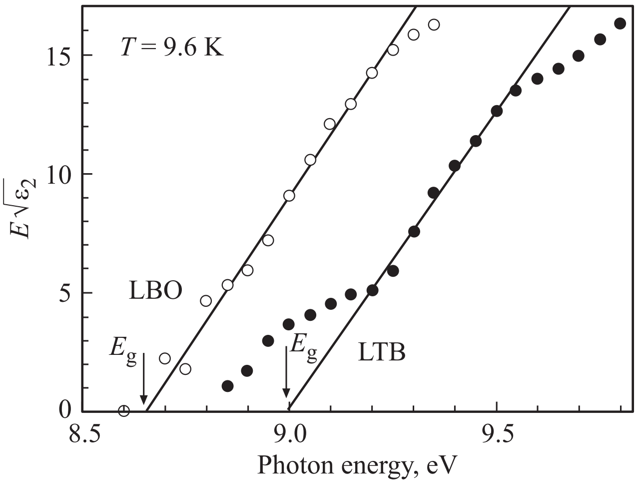

Figure 4. Fundamental absorption edge of LTB and LBO crystals at $T = 9.6\,\mathrm{K}$.

The observed dependence of ε_2 on the energy in the vicinity of the absorption edge indicates the indirect nature of electronic transitions. Extrapolation of the straight line to its intersection with the abscissa gives $E_g = 8.6-8.7\,\mathrm{eV}$ for LBO and $E_g = 8.8-8.9\,\mathrm{eV}$ for LTB. These values can be taken as an experimental estimate of the low-temperature band gap of LTB and LBO crystals. All the parameters obtained in this article, which characterize the absorption edge of each of the LTB and LBO crystals, are summarized in the table.

An increase in the lithium borates optical absorption at a photon energy above 7.5 eV should be considered to be caused by the fundamental absorption of the corresponding crystal at the edge. At the same time, the threshold of interband transitions E_g of lithium borates is located higher in the energy range from 8.5 to 8.9 eV (table). The lowest energy peak in the ε_2 spectrum appears in the region at $9.6-10\,\mathrm{eV}$ as an „arm“ on the low energy slope of the adjacent peak. Experimentally, this manifests itself in the fact that the LBO optical absorption increases sharply immediately above the fundamental absorption edge, which contrasts markedly with some other borates (for example, BBO, CBO), in which interband transitions at extreme points are symmetry forbidden and fundamental optical absorption becomes observable at energies well above the absorption edge [20]. A detailed examination of the lithium borates fundamental absorption edge at different temperatures (Fig. 1) indicates that it can be approximated quite well by the Lorentz curve, and the absorbance at the maximum of this absorption band can reach $10^4\,\mathrm{cm}^{-1}$. This is in complete agreement with the experimentally substantiated assumptions about the existence of exciton-like electronic excitations near the lithium borates fundamental absorption edge [9,33], which probably overlap with interband transitions.

Parameters of the fundamental VUV-absorption edge at $T = 293$ K and an estimate of the low-temperature band gap E_g at $T = 10$ K

Crystal	λ_c, nm	E_1, eV	E_2, eV	E_g, eV	E_{ε_2}, eV	$\partial E/\partial T$, 10^{-4} eV/K	ΔT, K
LBO $\perp Y$	156	7.40	7.95	8.5–8.6	9.6–10	−4.7	80–293
LBO $\perp X$	159	7.30	7.78	8.6–8.7	9.6–10	−4.3	80–293
LTB	165	7.25	7.65	8.8–8.9	9.6–10	−3.0	10–293

Note λ_c — Cutoff wavelength (short-wavelength boundary of the optical transparency region); E_1 and E_2 are energies at which the absorption coefficient k is 3 and 50 cm^{-1} respectively; E_g is band gap; E_{ε_2} is energy position of the maximum of the low-energy peak in the $\varepsilon_2(E)$ spectrum; $\partial E/\partial T$ is absorption edge temperature shift coefficient measured in the temperature range ΔT.

5. Conclusion

In this article, an experimental study of the VUV-edge of the fundamental optical absorption of lithium triborate LiB_3O_5 crystals of two crystal-lattice orientations (LBO $\perp Y$, LBO $\perp Y$) and non-oriented crystals of lithium tetraborate $Li_2B_4O_7$ (LTB) is performed. A set of parameters characterizing the VUV-fundamental absorption edge of lithium borates is obtained. Based on the recorded transmission ($T = 293$ K) and absorption ($T = 80$, 293 K) spectra, the short-wavelength boundary of the transparency band (cutoff wavelength) was determined; the energy position of the fundamental absorption edge at which the absorption coefficient $k = 50\,cm^{-1}$; absorption edge temperature shift coefficient $-(3–4.7) \cdot 10^{-4}$ eV/K. The dependence of the LBO absorption edge parameters on the crystal-lattice orientation is studied. Based on the low-temperature reflection spectra ($T = 10$ K, $\theta = 17°$, $E = 4–32$ eV), the Kramers–Kronig method was used to calculate the spectra optical constants: refraction (n) and absorption (k) indices, real (ε_1) and imaginary (ε_2) parts of the complex permittivity, and absorption coefficient μ. In the $\varepsilon_2(E)$ spectrum, the lowest-energy peak caused by electronic transitions from the valence band top to states at the conduction band bottom was studied, and the thresholds of interband transitions were determined (E_g at $T = 10$ K): 8.5–8.6 eV (LBO $\perp Y$), 8.6–8.7 eV (LBO $\perp X$) and 8.8–8.9 eV (LTB). The lowest-energy electronic transition in lithium borates, which determines the threshold E_g of the interband transitions onset, occurs between the states of the corresponding anionic group, which determines the valence band top and the conduction band bottom. In the region of the lithium borates fundamental absorption edge, no experimental manifestations of electronic transitions involving states of lithium cations have been identified.

Acknowledgments

The author is grateful to L.I. Isaenko for providing the crystals for the study, and to V.A. Pustovarov for his interest in the work and assistance in measurements in the VUV-region of the spectrum.

Conflict of interest

The author declares that he has no conflict of interest.

References

[1] A.N. Vasilev, V.V. Mikhaylin. Vvedeniye v spektroskopiyu dielektrikov. Yanus-K, M. (2000). 415 p. (in Russian).

[2] Yu.I. Ukhanov. Opticheskie svoistva poluprovodnikov. Nauka, M. (1977) 366 p. (in Russian).

[3] T.T. Tran, H. Yu, J.M. Rondinelli, K.R. Poeppelmeier, P.S. Halasyamani. Chem. Mater. **28**, 5238 (2016).

[4] Ya.V. Burak, Ya.O. Dovgii, I.V. Kityk. Optika i spektroskopiya, **69**, 1183 (1990) (in Russian).

[5] Ya.V. Burak, Ya.O. Dovgii, I.V. Kityk. FTT, **31**, 275 (1989) (in Russian).

[6] V.N. Kolobanov, J. Becker, S. Downes, B.I. Zadneprovsky, I.A. Kamenskikh, A. Karl, V.V. Mikhaylin, V.A. Nefedov, M. Runne, D. Tihan, I.N. Shpinkov, G. Tzimmerer. Tverdotelnyye detektory ioniziruyushchikh izlucheniy. 1-yy Vseros. simpozium TTD-97. Ekaterinburg (1997) P. 94. (in Russian).

[7] T.-J. Chen, R. Tao, J.C. Rife, W.R. Hunter. J. Opt. Soc. Am. B-Opt. Phys. **15**, 47 (1998).

[8] L.I. Isaenko, A.P. Yelisseyev. Chem. Sust. Dev. **8**, 213 (2000).

[9] I.N. Ogorodnikov, V.A. Pustovarov, A.V. Kruzhalov, L.I. Isaenko, M. Kirm, G. Zimmerer. FTT, **42**, 454 (2000) (in Russian).

[10] Ya.V. Burak, G.M. Gitskailo, I.T. Lyseiko, N.S. Pidzyrailo, I.V. Stefansky. Ukr. Fiz. Zh. **32**, 1509 (1987) (in Russian).

[11] B. Wu, N. Chen, C. Chen, D. Deng, Z. Xu. Opt. Lett. **14**, 1080 (1989).

[12] K. Kato. IEEE J. Quantum Electron. **26**, 1173 (1990).

[13] C. Chen, Y. Wu, A. Jiang, B. Wu, G. You, R.K. Li, S. Lin. J. Opt. Soc. Am. B-Opt. Phys. **6**, 616 (1989).

[14] I.N. Ogorodnikov, V.Yu. Ivanov, A.A. Maslakov, A.Yu. Kuznetsov, V.A. Maslov. Pisma v ZhTF, **19**, 42 (1993) (in Russian)

[15] I.N. Ogorodnikov, E.A. Radzhabov, L.I. Isaenko, A.V. Kruzhalov. FTT, **41**, 223 (1999) (in Russian).

[16] R. Komatsu, T. Sugawara, K. Sassa, N. Sarukura, Z. Liu, S. Izumida, Y. Segawa, S. Ida, T. Fukuda, K. Yamanouchi. Appl. Phys. Lett. **70**, 3492 (1997).

[17] V.V. Sobolev, V.V. Nemoshkalenko. Metody vychislitelnoy fiziki v teorii tverdogo tela. Elektronnaya struktura poluprovodnikov. Nauk. dumka, Kiev (1988). 424 p. (in Russian).

[18] D. Pines. Elementarnyye vozbuzhdeniya v tverdykh telakh. Mir, M. (1965). 382 pp. (in Russian)

[19] J. Li, C.-G. Duan, Z.-Q. Gu, D.-S. Wang, Phys. Rev. B: Condens. Matter **57**, 6925 (1998).
[20] R.H. French, J.W. Ling, F.S. Ohuchi, C.T. Chen. Phys. Rev. B: Condens. Matter **44**, 8496 (1991).
[21] W.Y. Hsu, R.V. Kasowski. J. Appl. Phys. **73**, 4101 (1993).
[22] Y.-N. Xu, W.Y. Ching. Phys. Rev. B: Condens. Matter **41**, 5471 (1990).
[23] N.A. Sobolev. FTT, **36**, 2926 (1994) (in Russian).
[24] A.B. Sobolev, A.Yu. Kuznetsov, I.N. Ogorodnikov, A.V. Kruzhalov. FTT, **36**, 1517 (1994) (in Russian).
[25] A.Yu. Kuznetsov, L.I. Isaenko, A.V. Kruzhalov, I.N. Ogorodnikov, A.B. Sobolev. FTT, **41**, 57 (1999) (in Russian).
[26] A.Yu. Kuznetsov, M.V. Kuznetsov, I.N. Ogorodnikov, A.V. Kruzhalov, V.A. Maslov. FTT, **36**, 845 (1994) (in Russian).
[27] Ch.B. Lushchik, A.Ch. Lushchik. Raspad elektronnykh vozbuzhdeniy s obrazovaniyem defektov v tverdykh telakh. Nauka, M. (1989). 264 p. (in Russian).
[28] I.N. Ogorodnikov, A.V. Porotnikov, V.A. Pustovarov, A.V. Kruzhalov. J. Lumin. **72**–**74**, 703 (1997).
[29] V. Kisand, R. Kink, M. Kink, J. Maksimov, M. Kirm, I. Martinson. Phys. Scripta **54**, 542 (1996).
[30] D. Visser, G.C. Verschoor, D.J.W. IJdo. Acta Crystallogr. **B36**, 28 (1980).
[31] T.-J. Chen, R.N. Zitter, R. Tao, W.R. Hunter, J.C. Rife. Phys. Rev. B: Condens. Matter **52**, 13703 (1995).
[32] J. Tauc, R. Grigorovici, A. Vancu. Phys. Status Solidi B **15**, 627 (1966).
[33] O.T. Antonyak, Ya.V. Burak, I.T. Lyseiko, N.S. Pidzyrailo, Z.A. Khapko. Optika i spektroskopiya, **61**, 550 (1986) (in Russian).